Liposomal Delivery of MicroRNA-7–Expressing Plasmid Overcomes Epidermal Growth Factor Receptor Tyrosine Kinase Inhibitor-Resistance in Lung Cancer Cells

Kammei Rai[1)], Nagio Takigawa[1)], Sachio Ito[2)], Hiromi Kashihara[1)], Eiki Ichihara[1)], Tateji Yasuda[3)], Kenji Shimizu[2)], Mitsune Tanimoto[1)], Katsuyuki Kiura[1)]

Affiliations of authors:

1) Department of Hematology, Oncology and Respiratory Medicine, Okayama University Graduate School of Medicine, Dentistry and Pharmaceutical Sciences, Okayama, Japan.

2) Department of Molecular Genetics, Okayama University Graduate School of Medicine, Dentistry and Pharmaceutical Sciences, Okayama, Japan.

3) Department of Cell Chemistry, Okayama University Graduate School of Medicine, Dentistry and Pharmaceutical Sciences, Okayama, Japan.

Running title: EGFR oncogene addiction and micro RNA 7

Keywords: lung cancer, EGFR, oncogene addiction, microRNA 7, liposomal delivery

Grant Support

Ministry of Education, Culture, Sports, Science, and Technology, Japan grants 21590995 (N. Takigawa) and 21659209 (K. Kiura).

Correspondence to: Nagio Takigawa, MD, PhD; 2-5-1 Shikata-cho, Okayama 700-8558, Japan. Tel: +81-86-235-7227; Fax: +81-86-232-8226; E-mail: ntakigaw@md.okayama-u.ac.jp

Abstract

Epidermal growth factor receptor (EGFR)-tyrosine kinase inhibitors (TKI) have been strikingly effective in lung cancers harboring activating EGFR mutations. Unfortunately, the cancer cells eventually acquire resistance to EGFR-TKI. Approximately 50% of the acquired resistance involves a secondary T790M mutation. To overcome the resistance, we focused on EGFR suppression using microRNA-7 (miR-7), targeting multiple sites in the 3'-untranslated region of EGFR mRNA. Two EGFR-TKI-sensitive cell lines (PC-9 and H3255) and two EGFR-TKI-resistant cell lines harboring T790M (RPC-9 and H1975) were used. We constructed miR-7-2 containing miR-7-expressing plasmid. After transfection of the miR-7-expressing plasmid, using cationic liposomes, a quantitative polymerase chain reaction and dual luciferase assay were performed to examine the efficacy. The antiproliferative effect was evaluated using a cell count assay and xenograft model. Protein expression was examined by Western blotting. The miR-7 expression level of the transfectants was approximately 30-fold higher, and the luciferase activity was ablated by 92%. miR-7 significantly inhibited cell growth, not only in PC-9 and H3255, but also in RPC-9 and H1975. Expression of IRS-1, RAF-1, and EGFR was suppressed in the four cell lines. Injection of the miR-7-expressing plasmid revealed marked tumor regression in a mouse xenograft model using RPC-9 and H1975. EGFR, RAF-1, and IRS-1 were suppressed in the residual tumors. These findings indicate promising therapeutic applications of miR-7-expressing plasmids against EGFR

oncogene-addicted lung cancers, including T790M resistance by liposomal delivery.

Introduction

Epidermal growth factor receptor (EGFR) is overexpressed in more than 60% of human non-small cell lung cancer (NSCLC) samples (1). EGFR signaling is so essential for the initiation and progression of cancer that it has become the focus of molecular targeting therapy (2). EGFR-tyrosine kinase inhibitors (EGFR-TKI) have a striking effect in NSCLC with activating EGFR mutations, and longer progression-free survival has been observed if patients are treated with EGFR-TKI compared with conventional chemotherapy (3-5). This efficacy was attributed to blocking EGFR oncogene addiction (6-7). Unfortunately, approximately 50% of patients who initially respond to EGFR-TKI acquired resistance to EGFR-TKI due to an additional EGFR T790M mutation in exon 20 (8). Because the T790M mutation restores the affinity of ATP to the ATP binding site of mutated EGFR, the oncogene addiction by the EGFR pathway is presumed to be sustained in EGFR-TKI-resistant cells harboring the T790M mutation (9-10). Thus, a method of suppressing the restored EGFR pathway is needed to overcome the resistance caused by the T790M mutation.

To develop a new approach for the suppression of EGFR, we focused on microRNA, which is known to intrinsically suppress mRNA by pairing with the 3'-untranslated region (UTR) of the mRNA; the mRNA is finally translated into a target protein (11). Compared with conventional molecular targeting therapies, such as EGFR-TKI and anti-EGFR antibodies, microRNA is expected to be independent of unexpected conformational changes due to secondary mutations. In recent years, it has become apparent that microRNAs play crucial roles in carcinogenesis (12). Moreover, some microRNAs can work as tumor suppressors *in vitro* (13-14). The induction of overexpression of such microRNAs may contribute to suppression of the target protein (15). Different from short-interfering (si) RNA, microRNAs are expected to work as part of a network and could affect the components of the same pathway at multiple levels (14).

Using the TargetScan software, microRNA-7 (miR-7) was mathematically predicted to effectively suppress EGFR in three different sites (16). Here, we show the antiproliferative effect of miR-7 against EGFR-addicted lung cancer cells both *in vitro* and *in vivo*.

Materials and Methods

Cell culture and reagents

PC-9, H3255, H1975, and A549 cells were derived from adenocarcinoma of the lung. PC-9 cells were obtained from Immuno-Biological Laboratories (Takasaki, Gunma, Japan). H3255, H1975, and A549 cells were purchased from the American Type Culture Collection (Manassas, VA). Gefitinib-resistant RPC-9 cells were established using PC-9 by continuous exposure to gefitinib in our laboratory (17). PC-9 cells harboring EGFR delE746-A750 in exon 19 and H3255 cells harboring EGFR L858R in exon 21 were sensitive to EGFR-TKI. RPC-9 cells carrying delE746-A750 with T790M and H1975 carrying L858R with T790M were resistant to EGFR-TKI. A549 cells harbored wild-type EGFR. All cell lines were cultured at 37°C in 5% CO_2 using RPMI-1640 medium supplemented with 10% heat-inactivated fetal bovine serum and 100 U/mL penicillin-streptomycin.

Construction of miR-7 expressing plasmids

The pre-miR-7-2 site was cloned from DNA of RPC-9 cells with 50-base pair (bp) flanking sequences by polymerase chain reaction (PCR). The forward primer was 5′-ATTGGATCCCTGACCTGGTGGCGAGGGGA-3′, and the reverse primer was 5′-TTAAAGCTTAACACGTGGAAGGATAGCCA-3′. After double digestion with BamHI and HindIII, the fraction was inserted into pSilencer™4.1- CMV neo (Ambion, Austin, TX). All sequences were confirmed by direct sequencing.

Quantitative PCR of miR-7

Quantitative reverse transcription (RT)-PCR validated the miR-7 expression by the constructed plasmid, using TaqMan MicroRNA Assays (Applied Biosystems, Carlsbad, CA) following the manufacturer’s instructions. Briefly, RT reactions containing RNA samples (24 h after transfection), looped-primers, 1× buffer, reverse transcriptase, and RNase inhibitor were incubated for 30 min each at 16°C and at 42°C. Real-time PCR was performed on an AB 7300 Real-Time PCR System (Applied Biosystems). The PCR program was 10 min at 95ºC, 40 cycles of 15 sec at 95ºC and 60 sec at 60ºC. U44 was adopted as an internal control. Data were collected from four independent experiments.

Cell count assay

Each cell line was cultured in a 10-cm plate and divided equally into a 6-well plate, then combined and divided into paired wells again. After 24 h, they were transfected with miR-7-expressing plasmid or control scrambled microRNA-expressing plasmid following the manufacturer's instructions (Hokkaido System Science, Sapporo, Japan). Total cells were macroscopically observed and counted using vital staining with 0.6% Trypan Blue 72 h after incubation at 37ºC.

Dual luciferase assay

The dual luciferase assay was performed following the manufacturer's instructions (Promega Dual-Luciferase Reporter Assay System, Promega Corporation, Madison, WI). We constructed reporter plasmids by inserting full-length EGFR 3′-UTR into pTK-hRG-Luci. The cells were cultured in a 6-well plate and transfected with either plasmids expressing miR-7 or control expressing scrambled microRNA, with reporter plasmid and pOA-hRG-Luci as internal controls. Fluorescence was measured by a Turner Designs Model TD-20/20 Luminometer (Turner Designs, Sunnyvale, CA).

Injection of liposome-coated, miR-7-expressing plasmid into a mouse xenograft model

Female 7-week-old athymic mice were purchased from Charles River Laboratories Japan, Inc. All mice were provided with sterilized food and water and housed in a barrier facility under a 12/12-h light/dark cycle. Cancer cells (2×10^6) were subcutaneously injected into the backs of the mice. At 1 week after injection, mice harboring tumors with approximately 5-mm longitudinal diameters were randomly assigned into one of two groups (5 mice per group) that received 3 μg/body of miR-7-expressing plasmid or control scrambled microRNA-expressing plasmid using *in vivo* optimized cationic liposome complexes by direct injection, as reported previously (Hokkaido System Science) (18-20). Tumor volume ($\text{width}^2 \times \text{length}/2$) was determined twice per week until either the disappearance of the tumor or day 20.

Western blot analyses

Cells or frozen tissue were lysed in radioimmunoprecipitation assay buffer (1% Triton X-100, 0.1% SDS, 50 mmol/L Tris-HCl, pH 7.4, 150 mmol/L NaCl, 1 mmol/L EDTA, 1 mmol/L

EGTA, 10 mmol/L β-glycerolphosphate, 10 mmol/L NaF, and 1 mmol/L sodium orthovanadate containing protease inhibitor tablets (Roche Applied Sciences, Indianapolis, IN)). Proteins were separated by electrophoresis on polyacrylamide gels, transferred onto nitrocellulose membranes, and probed with specific antibodies, followed by detection with Enhanced Chemiluminescence Plus (GE Healthcare Biosciences, Pittsburgh, PA). All antibodies were used following the manufacturer's instructions (Cell Signaling Technology, Danvers, MA).

Apoptosis detection by Hoechst staining and Western blot analysis

Apoptosis in drug-treated cells was determined using the technique following previous reports (21-23). Briefly, all cells at 48 h after the transfection were collected and re-suspended in 100 μl of staining solution (70 μg/ml Hoechst 33342 and 100 μg/ml propidium iodide in phosphate-buffered saline) and incubated at 37 °C for 15 min. The stained cells were viewed in a fluorescence microscope, ZEISS Axioplan plus OLYMPUS DP-72 (OLYMPUS, Tokyo, Japan), with the appropriate filters so as to visualize simultaneously the blue fluorescence from Hoechst 33342 and the red fluorescence from propidium iodide. Normal viable cells fluorescent blue within the nucleus, and the apoptotic cells showed condensation of chromatin and formation of small masses of varying sizes. Necrotic cells stained pink, but these cells were swollen, and the chromatin was not condensed and fragmented as in apoptotic cells. Apoptosis in xenograft models was evaluated using

Western blot analysis and immunohistochemistry. Western blot analysis was performed using human specific cleaved poly ADP-ribose polymerase (PARP) (Asp214) antibody (Santa Cruz Biotechnology, Santa Cruz, CA).

Statistical Analysis

Data are represented as means with 95% confidence intervals (CIs). Statistical significance was determined with an unpaired Student's *t*-test. P values < 0.05 were considered to indicate statistical significance. All statistical tests were two-sided.

Results

miR-7 is overexpressed by liposomal delivery of plasmids

Constructed plasmids containing miR-7-2 were transfected using cationic liposomes. After transfection, miR-7 expression by RPC-9 and H1975 cells was significantly increased, by approximately 30-fold compared with each cell line transfected with control plasmids (P < 0.0000002 each). The mean expression ratios to control in RPC-9 and H1975 cells were 31.7 (95% CI: 30.1–33.4) and 27.7 (95% CI: 23.1–33.4), respectively (Fig. 1).

miR-7 transfection suppresses the EGFR expression by binding EGFR 3′UTR

miR-7 directly inhibits EGFR expression via its 3′-UTR. Using the TargetScan software, we assessed the complementarity of miR-7 *in silico* to the EGFR 3′-UTR and found three sites of seed matches (13, 16, 24) (Fig. 2A). To assess miR-7 inhibition of EGFR, RPC-9 cells were transfected with the constructed plasmid expressing either miR-7 or control plasmid. We tested the inhibitory ability of the plasmid by transfection with miR-7 activity reporter, a synthesized plasmid containing the full length of EGFR 3′-UTR combined with the luciferase gene. A dual luciferase assay showed aberrant inhibition of luciferase activity, by 92%. The mean relative luciferase activities in control and miR-7 were 255.5 (95% CI: 223.5–287.6) and 19.8 (95% CI: 10.3–29.2), respectively ($P < 0.001$; Fig. 2B). This indicates highly effective inhibition by miR-7 against the full length of EGFR 3′-UTR.

Plasmids expressing miR-7 have antiproliferative effects *in vitro* through the suppression of EGFR

To evaluate the efficacy of the constructed plasmid expressing miR-7, each cell line was transfected with cationic liposomes. The cell number was apparently reduced under microscopic observation. The numbers of transfected cell lines were significantly reduced 72 h after transfection (Fig. 3). Cell numbers ($\times 10^4$/mL) of control versus transfectants in PC-9, RPC-9, H3255, and H1975 cell lines, respectively, were 51.7 (95% CI: 38.9–64.4) versus 26.7 (95% CI: 18.3–35.0), 14.7 (95%

CI: 11.8–17.6) versus 9.3 (95% CI: 8.0–10.7), 4.8 (95% CI: 3.3–6.3) versus 2.1 (95% CI: 1.3–3.0), and 3.9 (95% CI: 2.7–5.2) versus 1.2 (95% CI: 0.8–1.6). All *P* values for the differences between the control and the transfectants were < 0.05.

We also transfected plasmids expressing miR-7 into A549 cells carrying wild-type EGFR and *K-RAS* mutations (25). There was no significant aberrant growth suppression in the cells (Fig. S1). We suggest that the oncogene addiction of EGFR plays an important role in miR-7 efficacy.

miR-7 suppresses EGFR-AKT pathway activation

Because miR-7 was proven to effectively suppress the expression of mRNA of total EGFR, it can also suppress its downstream signals, such as AKT (13, 26). Western blot analyses showed a direct inhibitory effect against total EGFR by miR-7, as well as the suppression of AKT phosphorylation (Fig. 4A).

miR-7 has multiple targeting effects, as predicted *in silico*

miR-7 was reported to suppress insulin receptor substrate-1 (IRS-1) and proto-oncogene serine/threonine-protein kinase (RAF-1), as predicted *in silico* (27). The inhibitory effects of total IRS-1 and RAF-1 by miR-7 were demonstrated to varying degrees in the 4 cell lines (Fig. 4B).

miR-7-expressing plasmid has antitumor effects against EGFR-TKI-resistant cell lines *in vivo* through multiple suppression of the EGFR-AKT and salvage pathway

The antitumor effect of plasmids expressing miR-7 was examined by *in vivo* liposomal delivery against mouse xenograft models. We selected a non-viral transfection method using cationic liposomes, which has been reported to effectively express plasmids in a mouse model of peritoneal dissemination (19). In the mouse xenograft models of RPC-9 cells, 60% of target tumors disappeared macroscopically, and tumor volume shrank significantly (Fig. 5A). Ratios (%) of tumor volume on day 18 to those on day 1 (control vs. miR-7) were 296.4 (95% CI: 190.8–402.0) versus 1.6 (95% CI: 0.008–3.1; P = 0.005), respectively (Fig. 5B). Additionally, the mouse xenograft models of H1975 showed significant tumor volume reduction by the same treatment. Ratios (%) of tumor volumes on day 19 to those on day 1 (control vs. miR-7) were 786.5 (95% CI: 416.9–1156.0) versus 154.0 (95% CI: 154.0–295.8; P = 0.049), respectively (Fig. 5C, D). Expression of EGFR, RAF-1, and IRS-1 in residual tumors was suppressed, even in the cells that survived after the treatment (Fig. 6).

miR-7 transfection induces apoptosis

Fig. S2 showed 48 h treatment of miR-7 resulted in the increase of apoptotic cells as well as necrotic cells in these four oncogene addicted cell lines. Percentage of apoptotic cell numbers (%) of control versus transfectants in PC-9, RPC-9, H3255, and H1975 cell lines, respectively, were 0 (95% CI: 0–0) versus 11.2 (95% CI: 9.16–13.3), 1.30 (95% CI: 0.62–1.97) versus 22.1 (95% CI:

18.5–25.6), 0 (95% CI: 0–0) versus 9.67 (95% CI: 9.01–10.3), and 2.22 (95% CI: 0.185–4.26) versus 13.5 (95% CI: 11.4–15.6). All P values for the differences between the control and the transfectants were < 0.05. The increase in the expression of cleaved PARP was observed even in the residual tumors in xenograft models (Fig. 6).

Discussion

To our knowledge, this is the first report showing that miR-7 caused a dramatic response in an EGFR-TKI-resistant lung cancer xenograft model. Regardless of T790M mutation status, using cationic liposomes to inhibit EGFR signaling by plasmids expressing miR-7 has great clinical significance, because it may overcome approximately 50% of acquired resistance to EGFR-TKIs in the clinic. In nature, miR-7 was thought to be strongly associated with both neural differentiation of embryo stem cells and the development of neural networks in embryos, although the mechanism remains to be clarified (28). The targets of miR-7 have been shown to be total EGFR (2 or 3 sites in the 3′-UTR of mRNA), IRS-1 (single site), and RAF-1 (2 sites) (13, 26-27), which have important roles in the activated EGFR pathway in various cancer cell lines (2, 29-30). We confirmed the suppression of the expression of these proteins in this study. Thus, multiple targeting inhibitory effects by miR-7 might be advantageous to prevent crosstalk with EGFR signaling.

Although the efficacy of EGFR siRNA or miR-7 against A549 cells by suppressing EGFR signaling has been reported, the efficacy may be limited because of escape in the signal transduction pathway, typically due to *K-RAS* activation (27, 31). In fact, miR-7 caused no significant growth inhibition in the A549 cells, even though moderate suppression of RAF downstream of *K-RAS* by miR-7 resulted in some degree of decreased survival. In contrast, miR-7 suppressed the growth of EGFR oncogene-addicted cells, regardless of the EGFR T790M mutation.

The let-7, one of the best-studied microRNA, was altered in human lung cancers. The reduced let-7 expression was significantly associated with shortened postoperative survival and that overexpression of let-7 results in the inhibition of lung cancer cell growth (32). The let-7g was confirmed to work against *K-RAS* which has crucial role in proliferation of lung cancer cells, especially in the cell lines with *K-RAS* mutations (33). Thus, we explored microRNA which could target EGFR directly and could suppress EGFR addicted cancers. Two groups reported that miR-7 had antitumor effects in glioblastoma cell lines (13) and breast cancer cell lines (26), and that the effect depended primarily on the suppression of total EGFR. In contrast, Chou *et al.* showed that miR-7 had the possibility of promoting tumorigenesis in EGFR wild-type cell lines through Ets transcriptional repression factor 1 suppression (34); however, there was no valid analysis on whether ectopic miR-7 was in fact overexpressed by lentiviral introduction. Moreover, the adopted CL1-5 cells had *TP53* mutations and were not driven by EGFR signaling (35-36). They also suggested that miR-7 was concomitantly overexpressed in EGFR-expressing lung cancer patients (37). We examined intrinsic miR-7 expression in EGFR-addicted cells and nonaddicted A549 cells, and found that intrinsic miR-7 was significantly more overexpressed in EGFR-addicted cells than in A549 cells (Fig. S3). Thus, we suspected that miR-7 was at least activated by EGFR in a positive feedback mechanism as suggested by Li *et al.* in their description of photoreceptor differentiation (38). However, in our experiments, ectopic miR-7 were obviously overexpressed (approximately 30-fold; Fig. 1), and under these conditions, miR-7 inhibited the cell growth of EGFR-addicted cell lines both *in vitro* and *in vivo*. Although there have been many problems in the realization of the multiple targeting effects of microRNA, targeting the crucial pathway by microRNA in selected cancers will be an Achilles' heel, similar to molecular targeting therapy by EGFR-TKI (39). Our results of apoptosis assays indicated this multiple targeting effect restored apoptotic pathway which previously caused by EGFR-TKI (7, 40-41).

Just before the submission of our article, Saydam *et al.* reported that transfection of precursor miR-7 inhibited schwannoma cell growth by targeting EGFR, p21-activated kinase 1, and associated cdc42 kinase 1 oncogenes, as well as tumor suppressor function, in a xenograft model by evaluating the implantation of schwannoma cells. However, the adopted schwannoma cells (HEI-193) had not been shown to be under EGFR oncogene addiction. Moreover, they used miR-7 before implantation of the cancer cells, but not after tumor formation (42). The evaluation of the degree of EGFR oncogene addiction in each malignant cell line is very important when we pursue the major role of the miR-7 in tumorigenesis or in tumor suppression, because miR-7 seems to have a strong correlation with EGFR regulation among its multiple targets. In our experiments, if the EGFR oncogene addiction was restored because of T790M mutation, the antitumor efficacy of miR-7 was evident even in the EGFR-TKI-resistant models.

Transfection by liposomes seems to be safer than that by viral vectors, although some conditions should be optimized (43-44). The adopted cationic liposome and the constructed plasmid appears to have high microRNA expression efficiency, compared with results in a previous report (45). To our knowledge, this is the first report to show a dramatic effect of miR-7 against EGFR-TKI-resistant lung cancer cells *in vivo*. It suggests that the delivery of plasmids expressing miR-7 by cationic liposomes has therapeutic potential for overcoming acquired resistance to EGFR-TKI, and that a novel approach in RNA levels to overcome the resistance caused by secondary mutations in EGFR-addicted tumors might be warranted.

Acknowledgments

We thank Hokkaido Systems Science Co., Ltd. for the kind gifts of cationic liposomes and appropriate advice regarding efficient transfection. We used ZEISS Axioplan plus OLYMPUS DP-72 in Central Research Laboratory, Okayama University.

References

1. Jones RB, Gordus A, Krall JA, MacBeath G. A quantitative protein interaction network for the ErbB receptors using protein microarrays. Nature. 2006;439:168-74.

2. Herbst RS, Fukuoka M, Baselga J. Gefitinib--a novel targeted approach to treating cancer. Nat Rev Cancer. 2004;4:956-65.

3. Mitsudomi T, Morita S, Yatabe Y, Negoro S, Okamoto I, Tsurutani J, et al. Gefitinib versus cisplatin plus docetaxel in patients with non-small-cell lung cancer harbouring mutations of the epidermal growth factor receptor (WJTOG3405): an open label, randomised phase 3 trial. Lancet Oncol. 2010;11:121-8.

4. Maemondo M, Inoue A, Kobayashi K, Sugawara S, Oizumi S, Isobe H, et al. Gefitinib or chemotherapy for non-small-cell lung cancer with mutated EGFR. N Engl J Med. 2010;362:2380-8.

5. Mok TS, Wu YL, Thongprasert S, Yang CH, Chu DT, Saijo N, et al. Gefitinib or carboplatin-paclitaxel in pulmonary adenocarcinoma. N Engl J Med. 2009;361:947-57.

6. Haber DA, Bell DW, Sordella R, Kwak EL, Godin-Heymann N, Sharma SV, et al. Molecular targeted therapy of lung cancer: EGFR mutations and response to EGFR inhibitors. Cold Spring Harb Symp Quant Biol. 2005;70:419-26.

7. Sordella R, Bell DW, Haber DA, Settleman J. Gefitinib-sensitizing EGFR mutations in lung cancer activate anti-apoptotic pathways. Science. 2004;305:1163-7.

8. Toyooka S, Kiura K, Mitsudomi T. EGFR mutation and response of lung cancer to gefitinib. N Engl J Med. 2005;352:2136; author reply

9. Godin-Heymann N, Bryant I, Rivera MN, Ulkus L, Bell DW, Riese DJ, 2nd, et al. Oncogenic activity of epidermal growth factor receptor kinase mutant alleles is enhanced by the T790M drug resistance mutation. Cancer Res. 2007;67:7319-26.

10. Pao W, Miller VA, Politi KA, Riely GJ, Somwar R, Zakowski MF, et al. Acquired resistance of lung adenocarcinomas to gefitinib or erlotinib is associated with a second mutation in the EGFR kinase domain. PLoS Med. 2005;2:e73.

11. Lai EC. Micro RNAs are complementary to 3' UTR sequence motifs that mediate negative post-transcriptional regulation. Nat Genet. 2002;30:363-4.

12. Iorio MV, Croce CM. MicroRNAs in cancer: small molecules with a huge impact. J Clin Oncol. 2009;27:5848-56.

13. Kefas B, Godlewski J, Comeau L, Li Y, Abounader R, Hawkinson M, et al. microRNA-7 inhibits the epidermal growth factor receptor and the Akt pathway and is down-regulated in glioblastoma. Cancer Res. 2008;68:3566-72.

14. Tong AW, Nemunaitis J. Modulation of miRNA activity in human cancer: a new paradigm for cancer gene therapy? Cancer Gene Ther. 2008;15:341-55.

15. Petri A, Lindow M, Kauppinen S. MicroRNA silencing in primates: towards development of novel therapeutics. Cancer Res. 2009;69:393-5.

16. Lewis BP, Burge CB, Bartel DP. Conserved seed pairing, often flanked by adenosines, indicates that thousands of human genes are microRNA targets. Cell. 2005;120:15-20.

17. Ogino A, Kitao H, Hirano S, Uchida A, Ishiai M, Kozuki T, et al. Emergence of epidermal growth factor receptor T790M mutation during chronic exposure to gefitinib in a non small cell lung cancer cell line. Cancer Res. 2007;67:7807-14.

18. Sato Y, Murase K, Kato J, Kobune M, Sato T, Kawano Y, et al. Resolution of liver cirrhosis using vitamin A-coupled liposomes to deliver siRNA against a collagen-specific chaperone. Nat Biotechnol. 2008;26:431-42.

19. Kikuchi A, Aoki Y, Sugaya S, Serikawa T, Takakuwa K, Tanaka K, et al. Development of novel cationic liposomes for efficient gene transfer into peritoneal disseminated tumor. Hum Gene Ther. 1999;10:947-55.

20. Tachibana R, Harashima H, Ide N, Ukitsu S, Ohta Y, Suzuki N, et al. Quantitative analysis of correlation between number of nuclear plasmids and gene expression activity after transfection with cationic liposomes. Pharm Res. 2002;19:377-81.

21. Muscarella DE, Rachlinski MK, Sotiriadis J, Bloom SE. Contribution of gene-specific lesions, DNA-replication-associated damage, and subsequent transcriptional inhibition in topoisomerase inhibitor-mediated apoptosis in lymphoma cells. Exp Cell Res. 1998;238:155-67.

22. Takigawa N, Vaziri SA, Grabowski DR, Chikamori K, Rybicki LR, Bukowski RM, et al. Proteasome inhibition with bortezomib enhances activity of topoisomerase I-targeting drugs by NF-kappaB-independent mechanisms. Anticancer Res. 2006;26:1869-76.

23. Tabata M, Tabata R, Grabowski DR, Bukowski RM, Ganapathi MK, Ganapathi R. Roles of NF-kappaB and 26 S proteasome in apoptotic cell death induced by topoisomerase I and II poisons in human nonsmall cell lung carcinoma. J Biol Chem. 2001;276:8029-36.

24. Griffiths-Jones S, Grocock RJ, van Dongen S, Bateman A, Enright AJ. miRBase: microRNA sequences, targets and gene nomenclature. Nucleic Acids Res. 2006;34:D140-4.

25. Valenzuela DM, Groffen J. Four human carcinoma cell lines with novel mutations in position 12 of c-K-ras oncogene. Nucleic Acids Res. 1986;14:843-52.

26. Reddy SD, Ohshiro K, Rayala SK, Kumar R. MicroRNA-7, a homeobox D10 target, inhibits p21-activated kinase 1 and regulates its functions. Cancer Res. 2008;68:8195-200.

27. Webster RJ, Giles KM, Price KJ, Zhang PM, Mattick JS, Leedman PJ. Regulation

of epidermal growth factor receptor signaling in human cancer cells by microRNA-7. J Biol Chem. 2009;284:5731-41.

28. Chen H, Shalom-Feuerstein R, Riley J, Zhang SD, Tucci P, Agostini M, et al. miR-7 and miR-214 are specifically expressed during neuroblastoma differentiation, cortical development and embryonic stem cells differentiation, and control neurite outgrowth in vitro. Biochem Biophys Res Commun. 2010;394:921-7.

29. Guix M, Faber AC, Wang SE, Olivares MG, Song Y, Qu S, et al. Acquired resistance to EGFR tyrosine kinase inhibitors in cancer cells is mediated by loss of IGF-binding proteins. J Clin Invest. 2008;118:2609-19.

30. Yamamoto T, Taya S, Kaibuchi K. Ras-induced transformation and signaling pathway. J Biochem. 1999;126:799-803.

31. Zhang M, Zhang X, Bai CX, Song XR, Chen J, Gao L, et al. Silencing the epidermal growth factor receptor gene with RNAi may be developed as a potential therapy for non small cell lung cancer. Genet Vaccines Ther. 2005;3:5.

32. Takamizawa J, Konishi H, Yanagisawa K, Tomida S, Osada H, Endoh H, et al. Reduced expression of the let-7 microRNAs in human lung cancers in association with shortened postoperative survival. Cancer Res. 2004;64:3753-6.

33. Kumar MS, Erkeland SJ, Pester RE, Chen CY, Ebert MS, Sharp PA, et al. Suppression of non-small cell lung tumor development by the let-7 microRNA family. Proc Natl Acad Sci U S A. 2008;105:3903-8.

34. Chou YT, Lin HH, Lien YC, Wang YH, Hong CF, Kao YR, et al. EGFR promotes lung tumorigenesis by activating miR-7 through a Ras/ERK/Myc pathway that targets the Ets2 transcriptional repressor ERF. Cancer Res. 2010;70:8822-31.

35. Chu YW, Yang PC, Yang SC, Shyu YC, Hendrix MJ, Wu R, et al. Selection of invasive and metastatic subpopulations from a human lung adenocarcinoma cell line. Am J Respir Cell Mol Biol. 1997;17:353-60.

36. Wang SP, Wang WL, Chang YL, Wu CT, Chao YC, Kao SH, et al. p53 controls cancer cell invasion by inducing the MDM2-mediated degradation of Slug. Nat Cell Biol. 2009;11:694-704.

37. Chou YT, Lin HH, Lien YC, Wang YH, Hong CF, Kao YR, et al. EGFR Promotes Lung Tumorigenesis by Activating miR-7 through a Ras/ERK/Myc Pathway that Targets the Ets2 Transcriptional Repressor ERF. Cancer Res. 2010.

38. Li X, Carthew RW. A microRNA mediates EGF receptor signaling and promotes photoreceptor differentiation in the Drosophila eye. Cell. 2005;123:1267-77.

39. Weinstein IB. Cancer. Addiction to oncogenes--the Achilles heal of cancer. Science. 2002;297:63-4.

40. Tracy S, Mukohara T, Hansen M, Meyerson M, Johnson BE, Janne PA. Gefitinib induces apoptosis in the EGFRL858R non-small-cell lung cancer cell line H3255. Cancer Res. 2004;64:7241-4.

41. Ling YH, Lin R, Perez-Soler R. Erlotinib induces mitochondrial-mediated apoptosis in human H3255 non-small-cell lung cancer cells with epidermal growth factor receptorL858R mutation through mitochondrial oxidative phosphorylation-dependent activation of BAX and BAK. Mol Pharmacol. 2008;74:793-806.

42. Saydam O, Senol O, Wurdinger T, Mizrak A, Ozdener GB, Stemmer-Rachamimov AO, et al. miRNA-7 attenuation in Schwannoma tumors stimulates growth by upregulating three oncogenic signaling pathways. Cancer Res. 2011;71:852-61.

43. Dass CR. Lipoplex-mediated delivery of nucleic acids: factors affecting in vivo transfection. J Mol Med. 2004;82:579-91.

44. Ma B, Zhang S, Jiang H, Zhao B, Lv H. Lipoplex morphologies and their influences on transfection efficiency in gene delivery. J Control Release. 2007;123:184-94.

45. Serikawa T, Suzuki N, Kikuchi H, Tanaka K, Kitagawa T. A new cationic liposome for efficient gene delivery with serum into cultured human cells: a quantitative analysis using two independent fluorescent probes. Biochim Biophys Acta. 2000;1467:419-30.

Figure legends

Figure 1

MicroRNA expression using liposomal delivery in EGFR-TKI-resistant cell lines. Quantitative polymerase chain reaction was performed, and expression of miR-7 was calculated by the ΔCt method in resistant cell lines. A plasmid expressing scrambled microRNA was used as a control. Means (bars) and 95% confidence intervals (error bars) are shown. (A) Ectopic miR-7 expression in RPC-9, which had an EGFR mutation delE746-A750 in exon 19 and T790M in exon 20. (B) Ectopic miR-7 expression in H1975, which had an EGFR mutation L858R in exon 21 and T790M in exon 20.

Figure 2

Inhibition of luciferase activity with synthesized EGFR 3'-UTR using liposomal delivery of miR-7-expressing plasmids. (A) Three match sites between miR-7 and the 3'-UTR of EGFR mRNA. (B) Relative luciferase activity in the RPC-9 cells 24 h after transfection of plasmids expressing miR-7 or scrambled microRNA as control. Means (bars) and 95% confidence intervals (error bars) are shown.

Figure 3

Antiproliferative effect of transfection of plasmids expressing miR-7. Upper panels, microscopic pictures of each cell line 72 h after transfection. Lower panels, the cell counts after transfection of miR-7-expressing plasmids or controls. Means (bars) and 95% confidence intervals (error bars) are shown.

Figure 4

Western blot analyses of the signal transduction pathway. β-actin was used as a loading control. (A) Western blot analyses of EGFR and phosphorylated protein kinase B (AKT) protein as the main stream of oncogene addiction in PC-9, RPC-9, H3255, and H1975 cells 60 h after transfection of plasmids expressing miR-7 or scrambled microRNA as a control. (B) Western blot analyses of insulin receptor substrate-1 (IRS-1) and proto-oncogene serine/threonine-protein kinase (RAF-1) as the salvage stream of oncogene addiction. Cleaved PARP seemed slightly increased.

Figure 5

Xenograft mice treated with miR-7. Mean tumor volumes (bars) and 95% confidence intervals (error bars) are shown. (A) Typical pictures of xenograft models (RPC-9). A plasmid expressing miR-7 (3 μg/body) was directly injected into tumors weekly in RPC-9 xenograft mice. Control mice were injected with control scrambled microRNA-expressing plasmids. (B) Growth curves of RPC-9 xenograft tumors. The relative percentage from original tumors was plotted. (C) Typical pictures of an H1975 xenograft model. (D) Growth curves of H1975 xenograft tumors.

Figure 6

Western blot analyses of the signal transduction pathway and apoptosis. Frozen tumors were obtained from RPC-9 and H1975 xenograft models at the end of the final tumor size evaluation. β-actin was used as a loading control. EGFR, phosphorylated protein kinase B (AKT), insulin receptor substrate-1 (IRS-1), proto-oncogene serine/threonine-protein kinase (RAF-1), and cleaved Poly ADP-ribose polymerase (PARP) were examined.

Figure S1

Effect of miR-7 overexpression in A549. (A) Cell counts 72 h after transfection of control scrambled microRNA-expressing or miR-7-expressing plasmids. Means (bars) and 95% confidence intervals (error bars) are shown. (B) Western blot analyses of EGFR, phosphorylated protein kinase B (AKT), insulin receptor substrate-1 (IRS-1), and proto-oncogene serine/threonine-protein kinase (RAF-1). β-actin was used as a loading control.

Figure S2

Apoptosis by miR-7 transfection. Upper panels, typical microscopic pictures of Hoechst staining 48 h after transfection. Scale bar indicate 100μm. Lower panels, the cell counts (%) of apoptotic and necrotic cells after transfection of miR-7-expressing plasmids or controls. Means (bars) and 95% confidence intervals (error bars) are shown.

Figure S3

Intrinsic miR-7 expression in each cell line. Means (bars) and 95% confidence intervals (error bars) are shown.

The English in this document has been checked by at least two professional editors, both native speakers of English. For a certificate, please see:

http://www.textcheck.com/certificate/vlgAnA

http://www.textcheck.com/certificate/gi2fPx

A

	miR-7Ct	U44Ct	” Ct miR-7Ct-U44Ct	⊿⊿Ct ⊿CtControl-⊿Ct miR-7p	$2^{-⊿⊿Ct}$
Control	25.002675(±0.23071)	18.904(±0.059594)	6.0986(±0.22960)	0.0000 (±0.22960)	1(0.85287-1.1725)
miR-7 expressing plasmid (miR-7p)	18.834(±0.57568)	17.721(±0.12687)	1.1132(±0.074743)	-4.98545(±0.074743)	31.678(30.079-33.363)

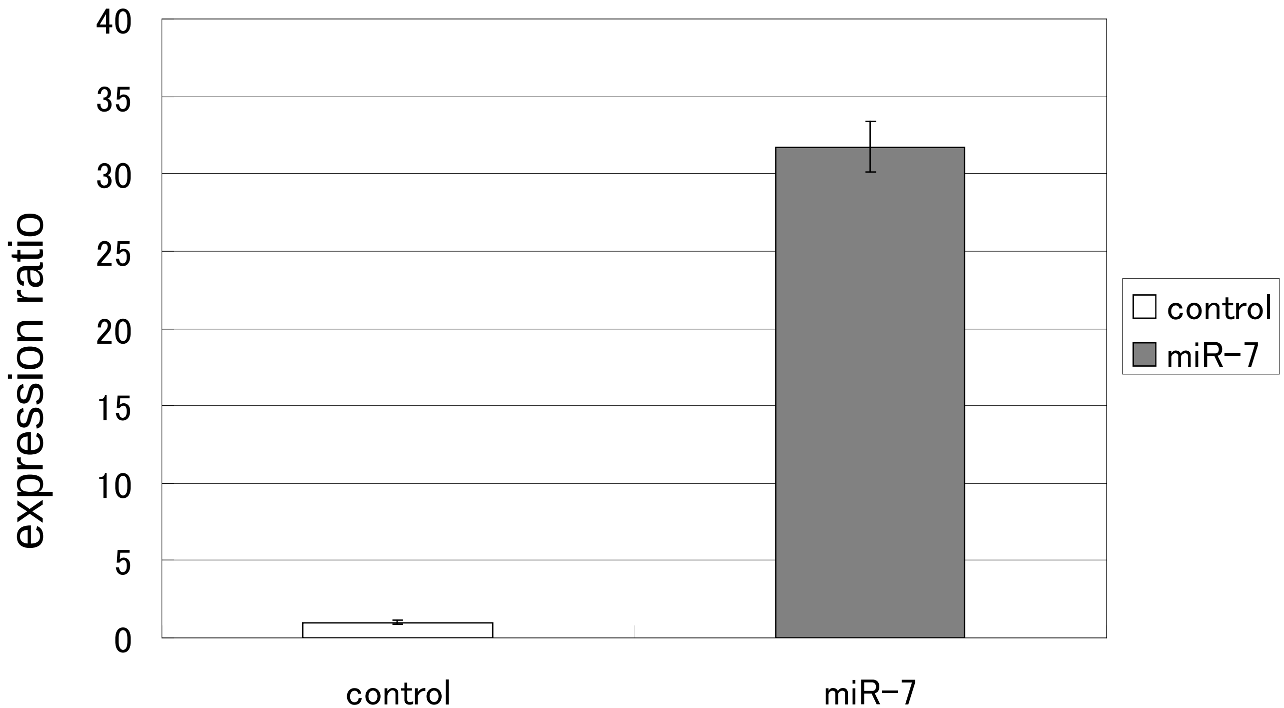

Figure 1

B

	miR-7Ct	U44Ct	” Ct miR-7Ct-U44Ct	⊿⊿Ct ⊿CtControl-⊿Ct miR-7p	$2^{-⊿⊿Ct}$
Control	26.803(±0.25012)	19.536(±0.075007)	7.2677(±0.20674)	0.0000 (±0.20674)	1(0.86649-1.15408)
miR-7 expressing plasmid (miR-7p)	21.709(±0.071756)	19.236(±0.32904)	2.4738(±0.26637)	-4.79385(±0.26637)	27.739(23.063-33.364)

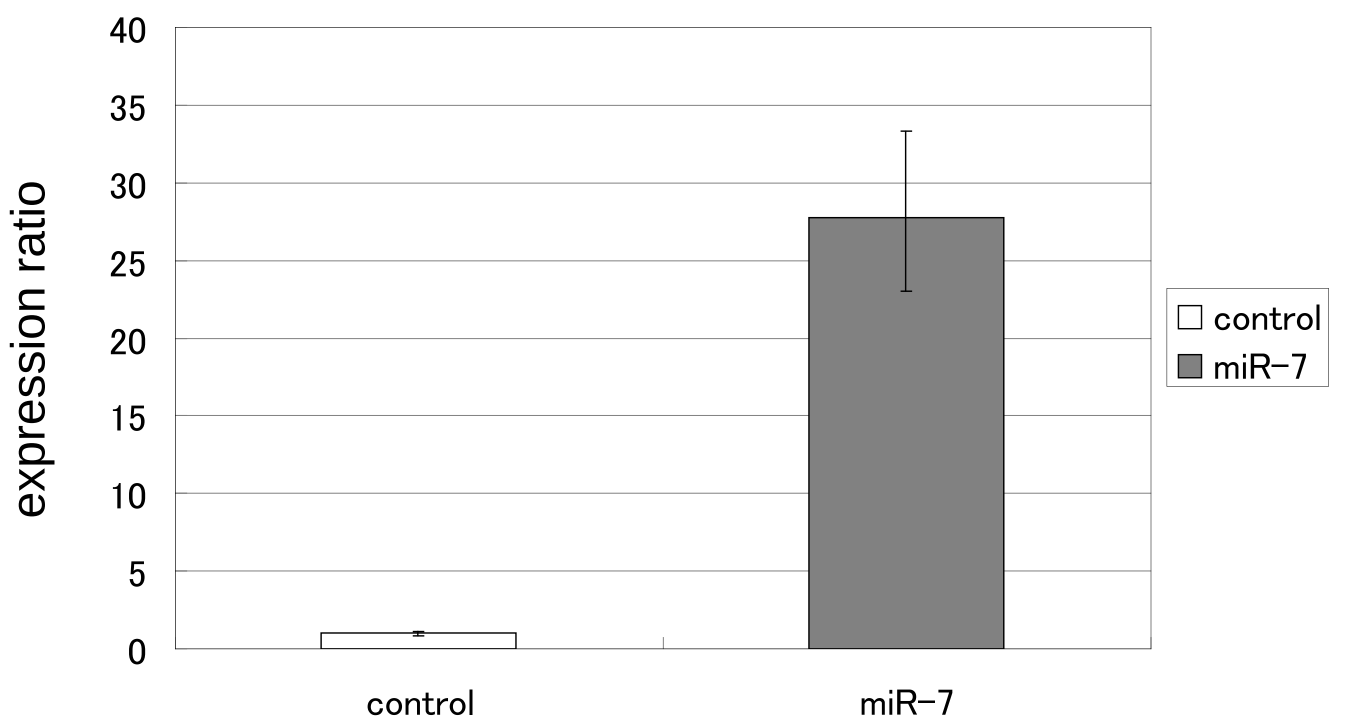

Figure 1

A


miR-7
U U G U U U U A G U G A U C A G A A G G U
G A C T G A C T T G T T T G T C T T C C A
EGFR 3’UTR region 442-464
miR-7
U U G U U U U A G U G A U C A G A A G G U
A C T T G A A T T G T T T G T C T T C C A
EGFR 3’UTR region 726-747
miR-7
GA
U U G U U U U A G U U C A G A A G G U
TT A C T T G A A T G G G C T C T T C C A
EGFR 3’UTR region 357-377

Figure 2

B

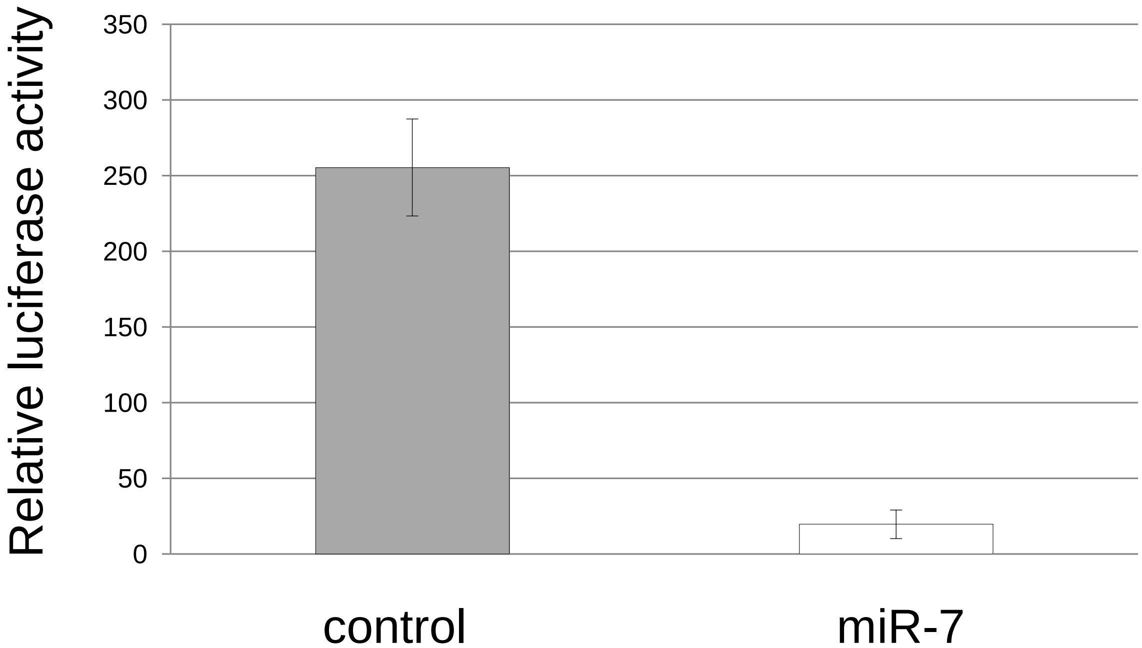
Relative luciferase activity
350
300
250
200
150
100
50
0
control
miR-7

Figure 2

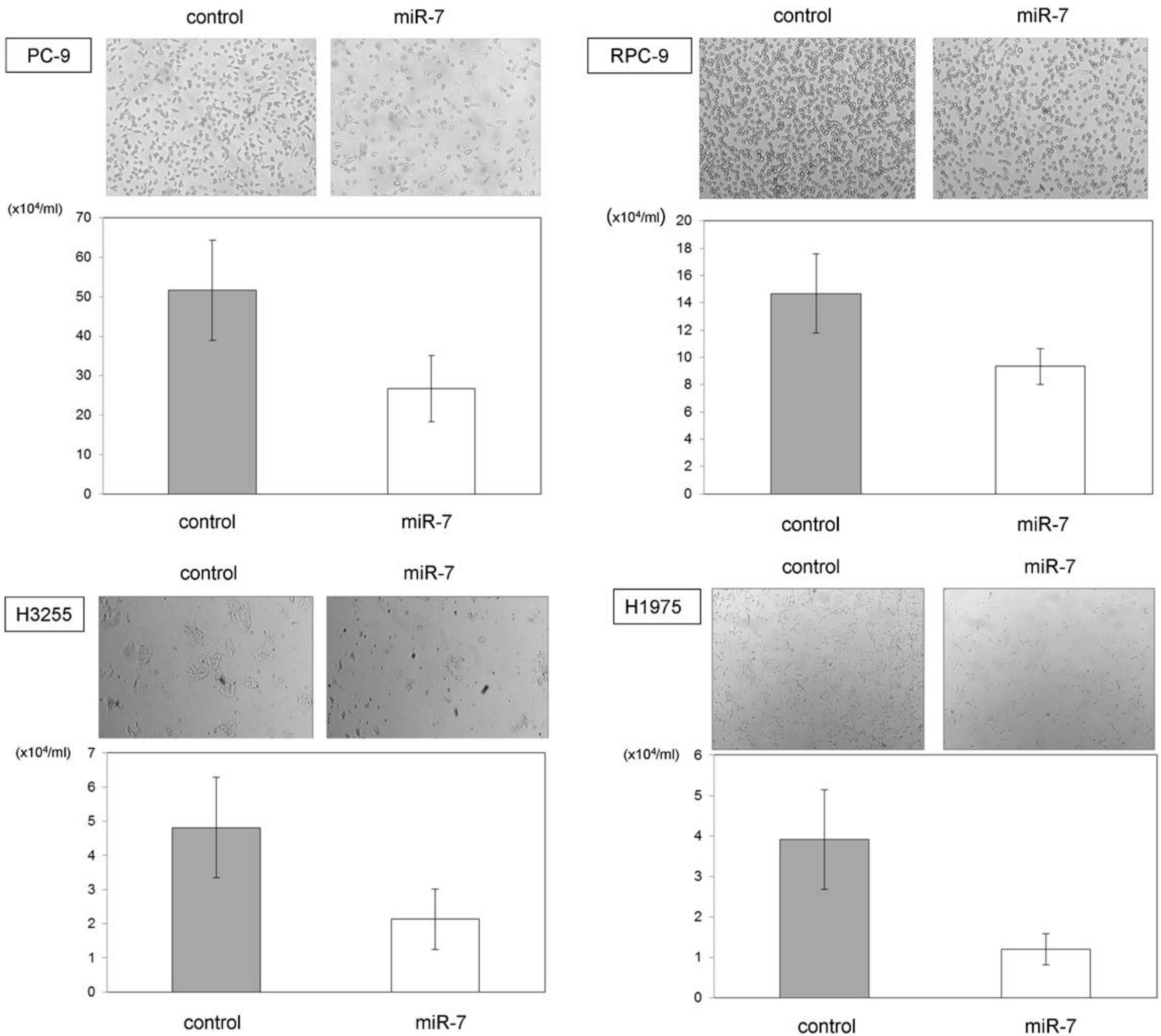

control
miR-7
PC-9
(x10⁴/ml)
70
60
50
40
30
20
10
0
control
miR-7
control
miR-7
RPC-9
(x10⁴/ml)
20
18
16
14
12
10
8
6
4
2
0
control
miR-7
control
miR-7
H3255
(x10⁴/ml)
7
6
5
4
3
2
1
0
control
miR-7
control
miR-7
H1975
(x10⁴/ml)
6
5
4
3
2
1
0
control
miR-7

Figure 3

A

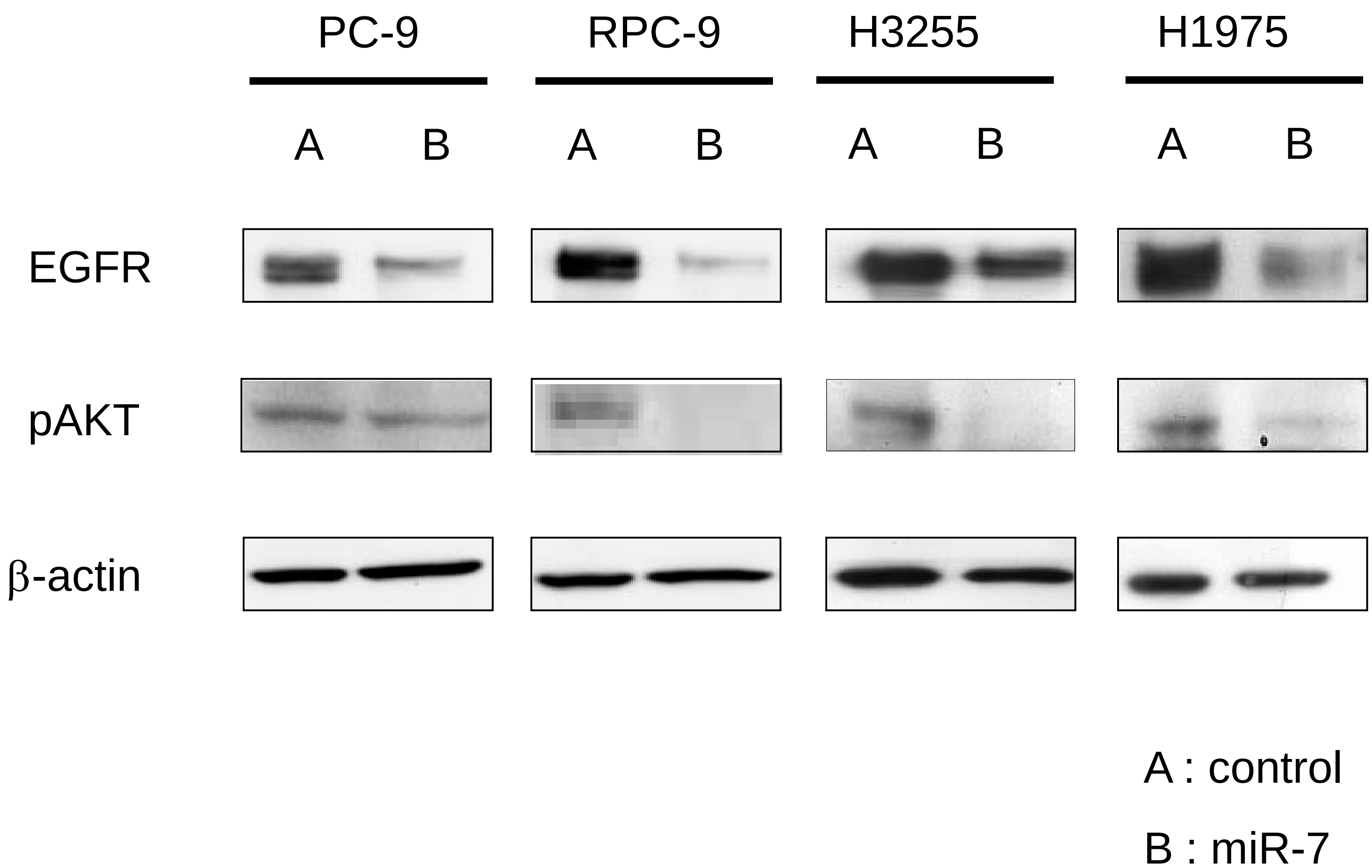
PC-9
RPC-9
H3255
H1975
A
B
A
B
A
B
A
B
EGFR
pAKT
β-actin
A : control
B : miR-7

Figure 4

B

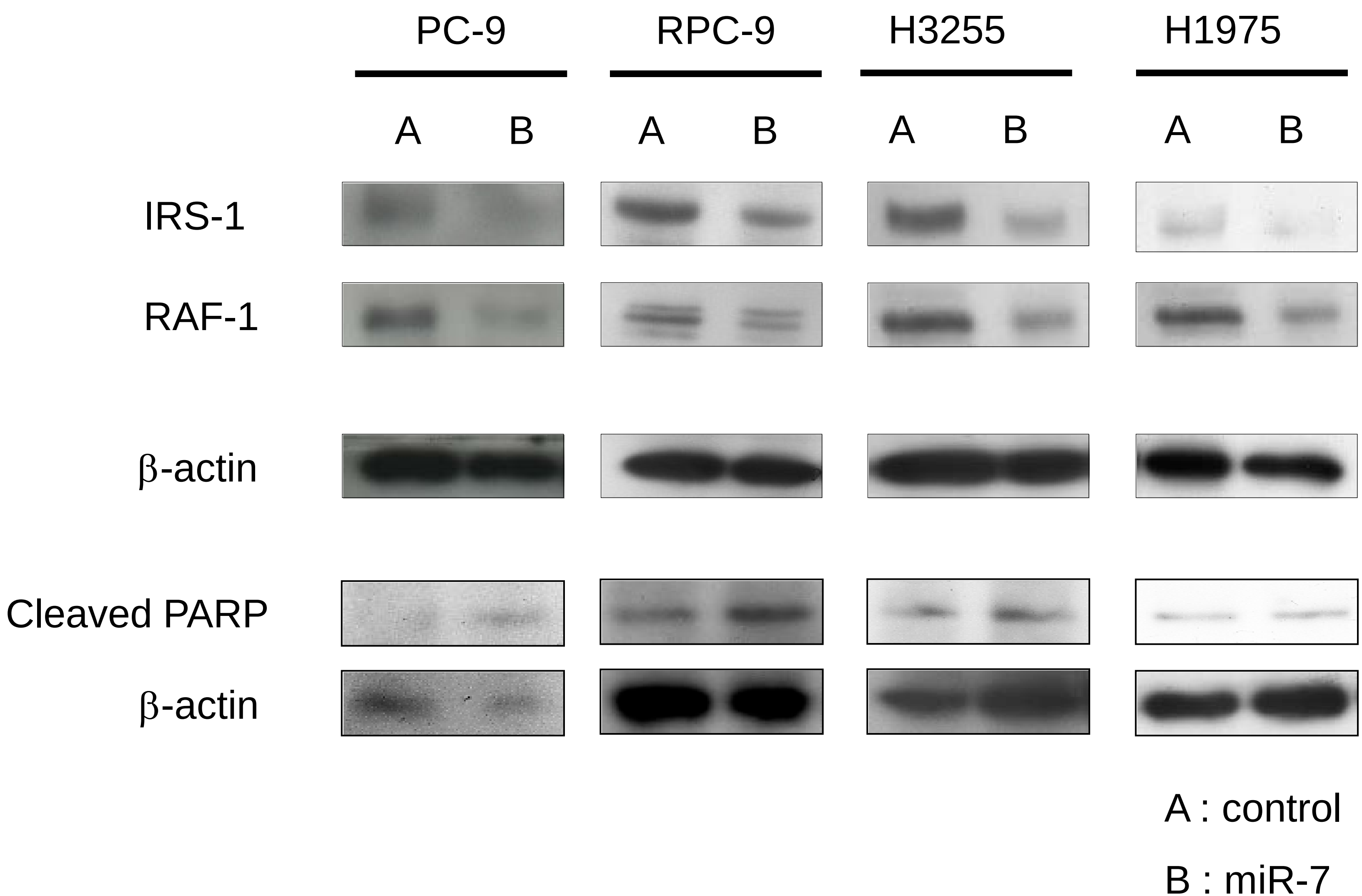

PC-9
RPC-9
H3255
H1975
A B A B A B A B
IRS-1
RAF-1
β-actin
Cleaved PARP
β-actin
A : control
B : miR-7

Figure 4

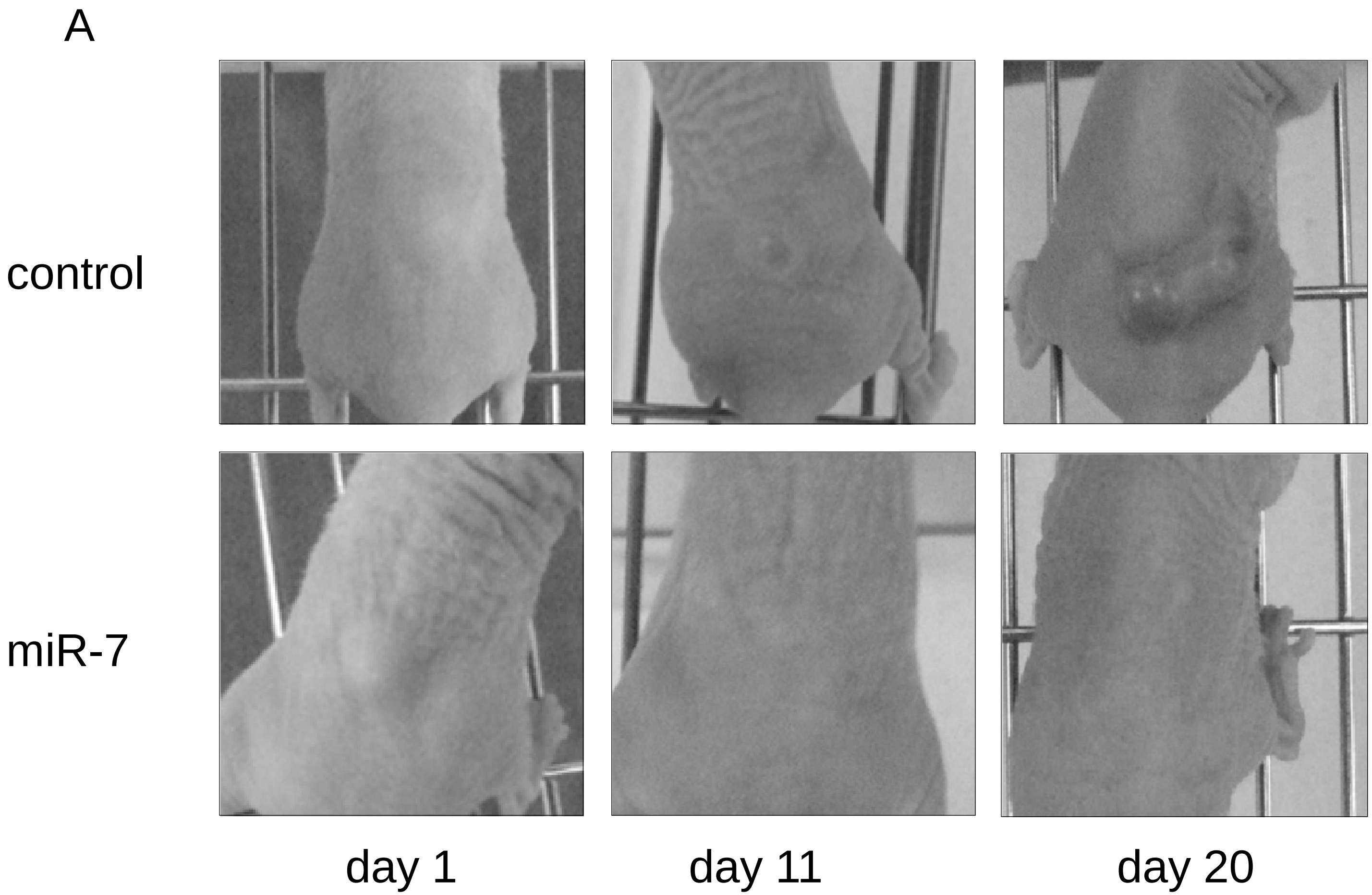

Figure 5

B

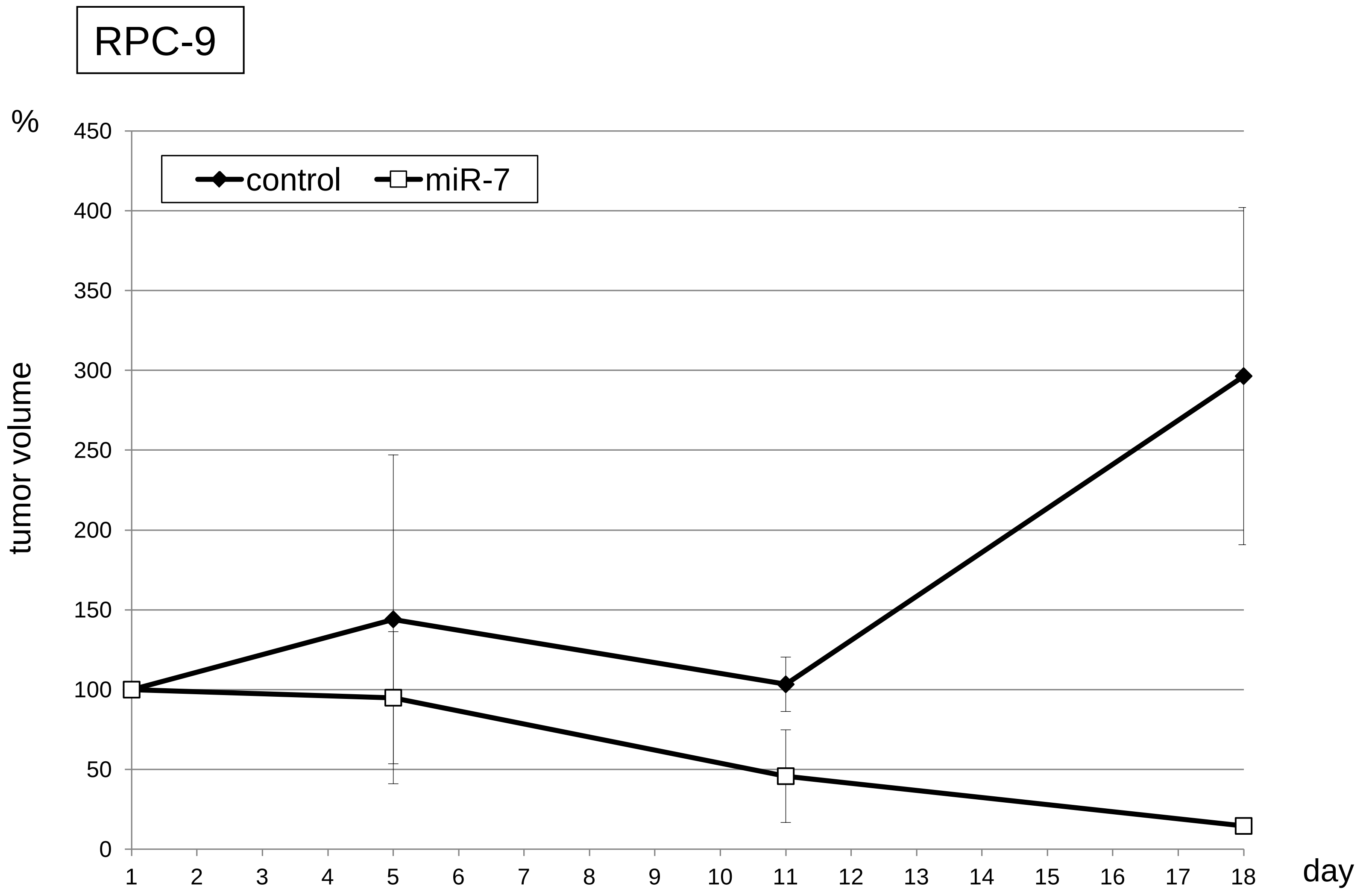
RPC-9
%
tumor volume
450
400
350
300
250
200
150
100
50
0
control
miR-7
1
2
3
4
5
6
7
8
9
10
11
12
13
14
15
16
17
18
day

Figure 5

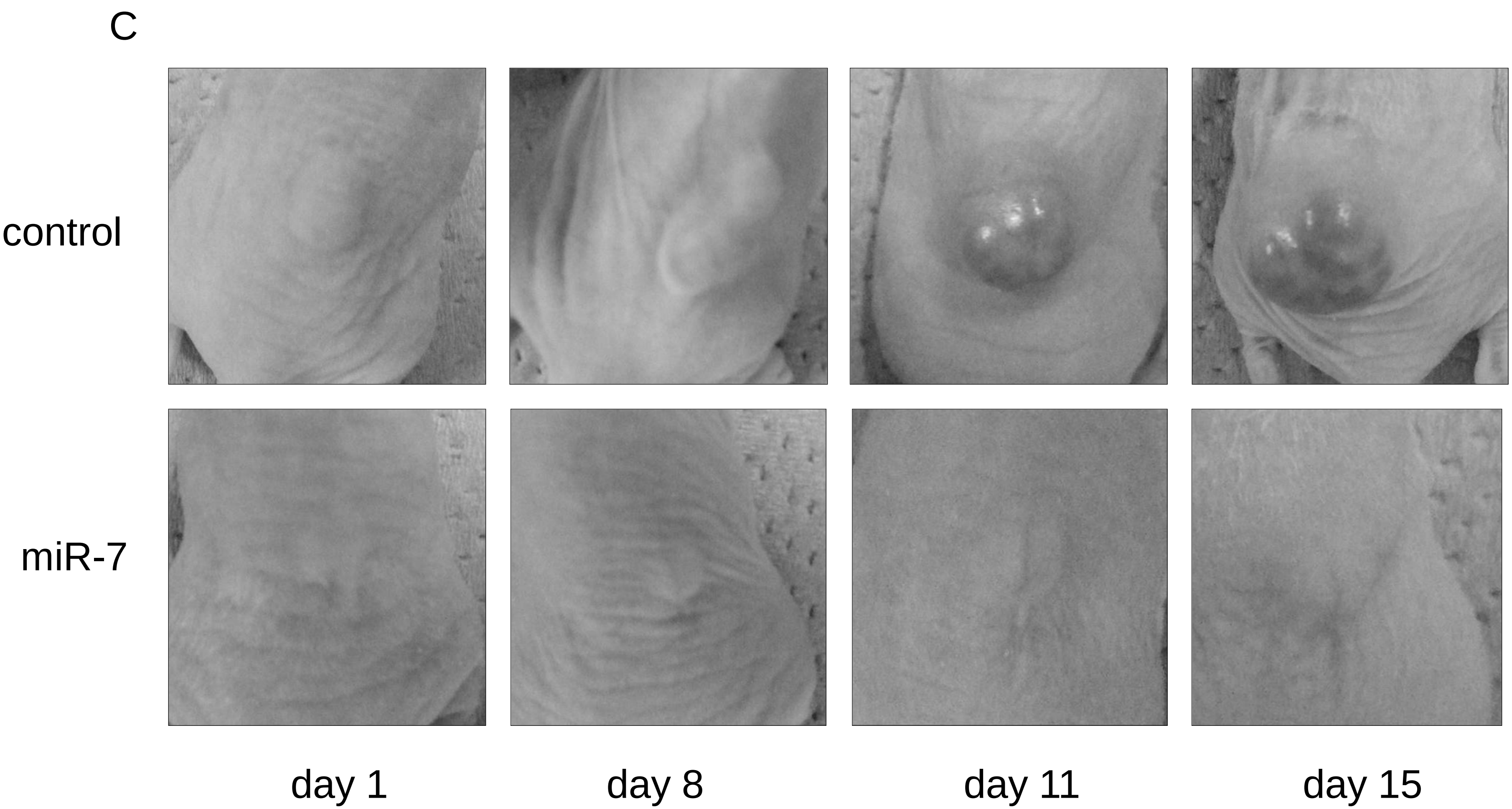

Figure 5

D

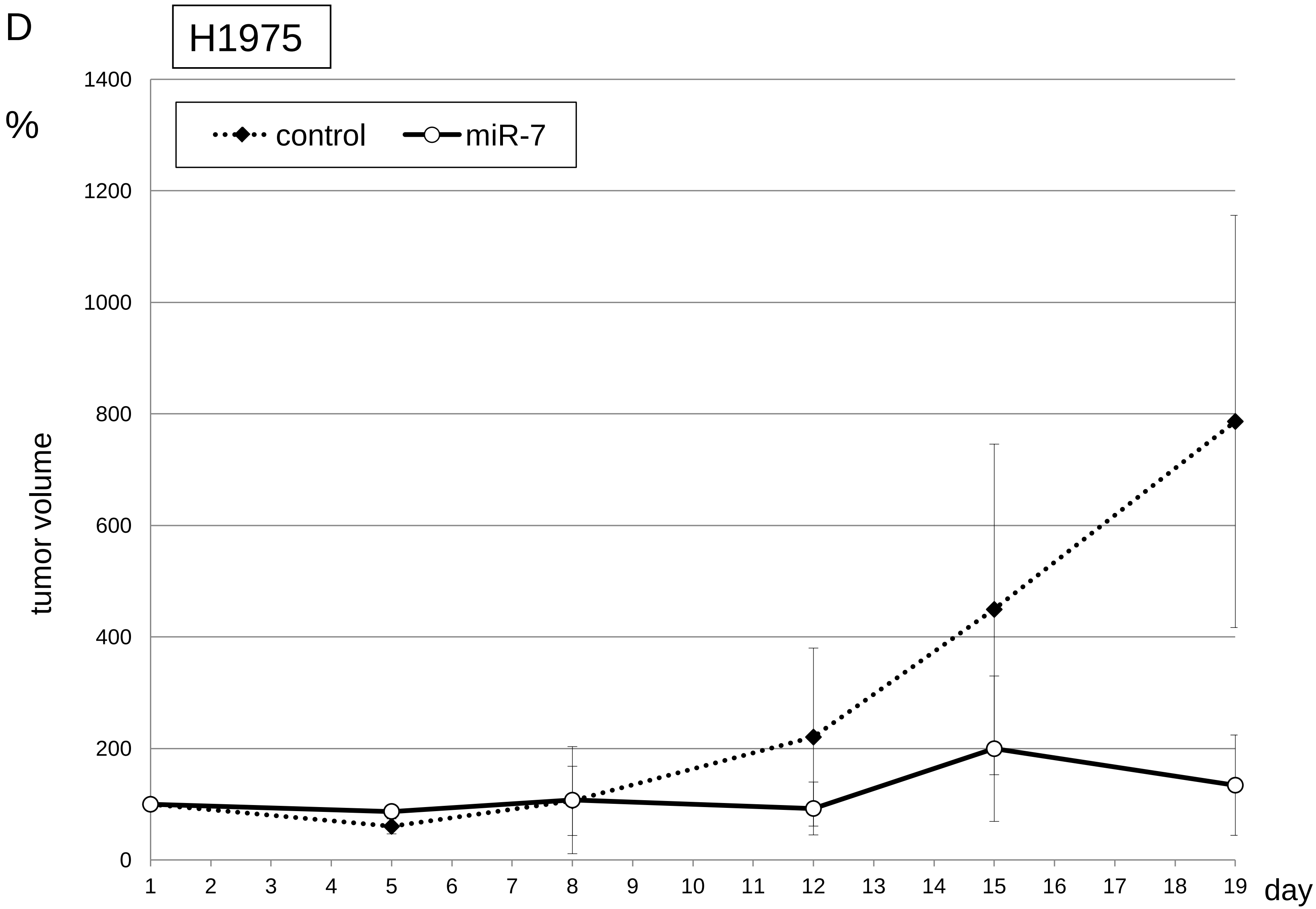
H1975
%
control
miR-7
tumor volume
1400
1200
1000
800
600
400
200
0
1
2
3
4
5
6
7
8
9
10
11
12
13
14
15
16
17
18
19
day

Figure 5

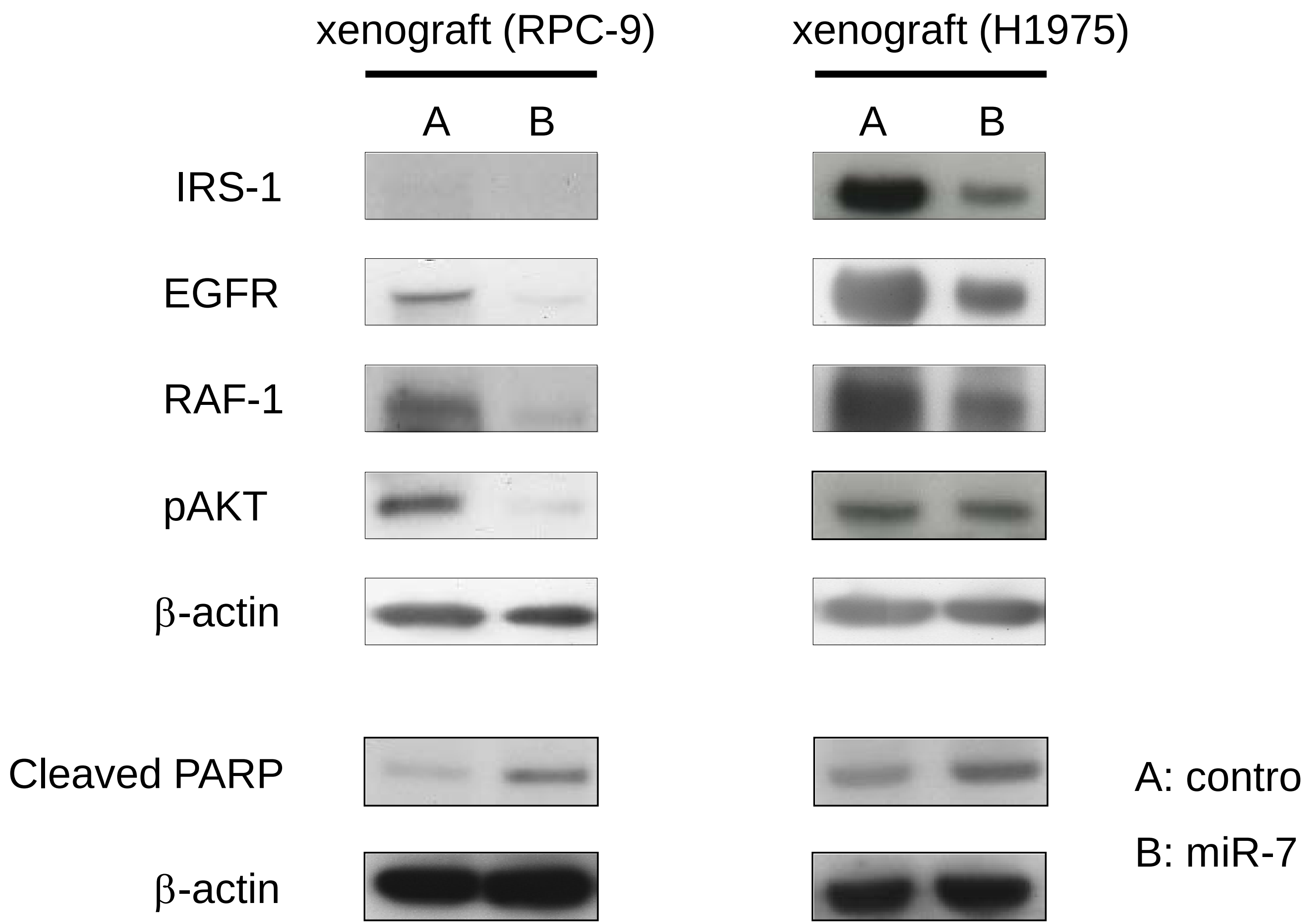
xenograft (RPC-9)
xenograft (H1975)
A
B
A
B
IRS-1
EGFR
RAF-1
pAKT
β-actin
Cleaved PARP
β-actin
A: control
B: miR-7

Figure 6

A

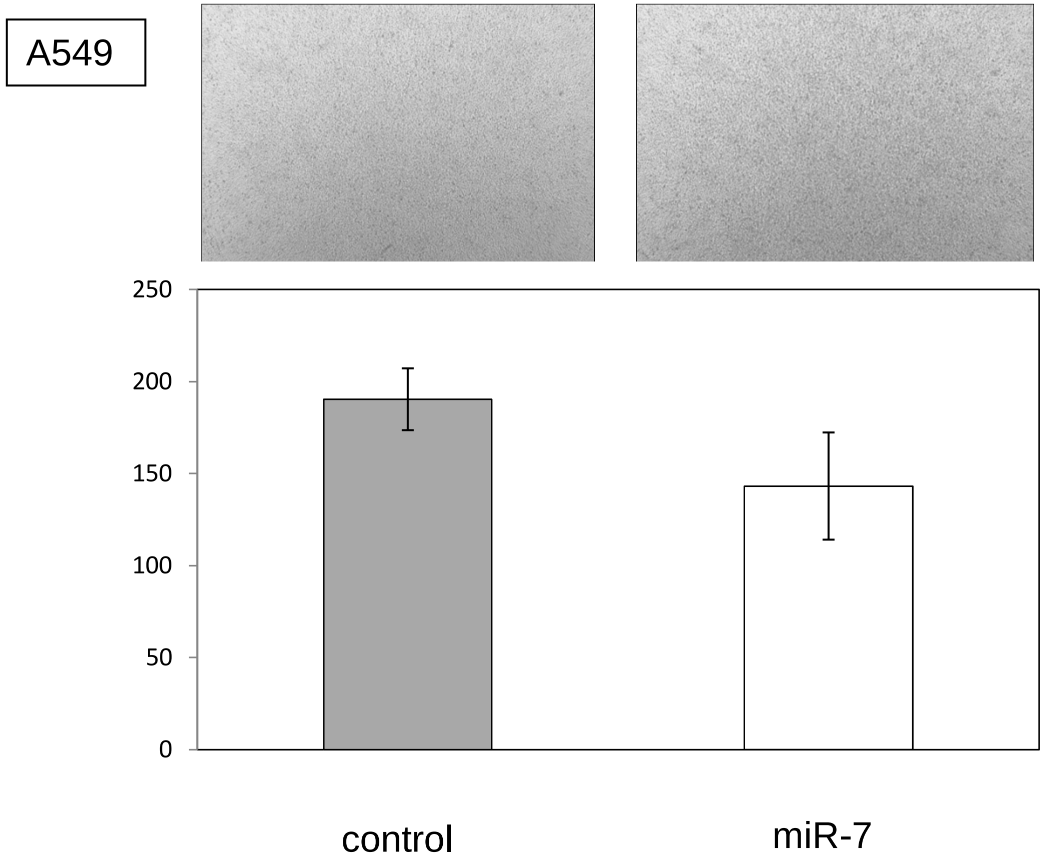

Figure S1

B

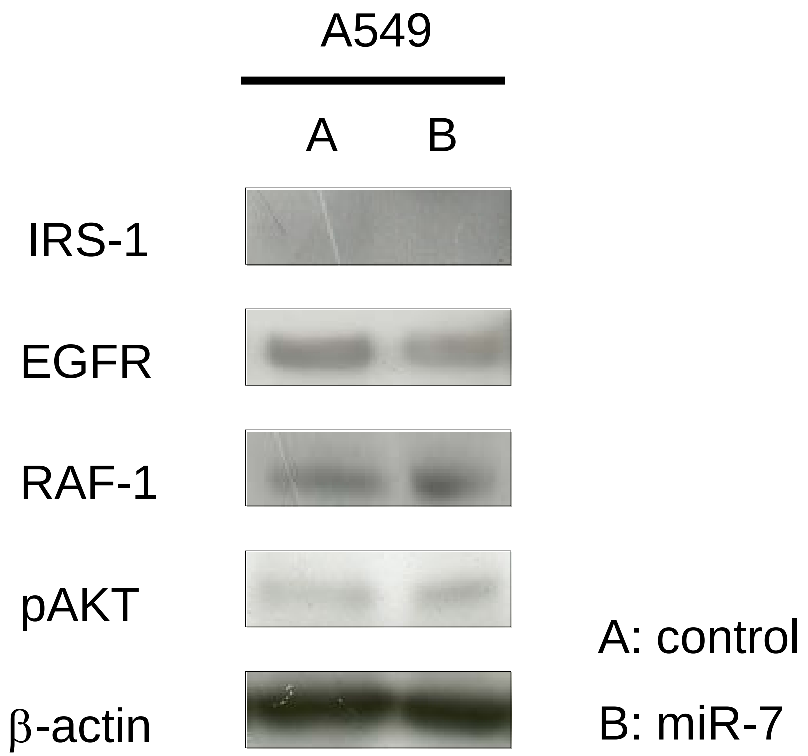

Figure S1

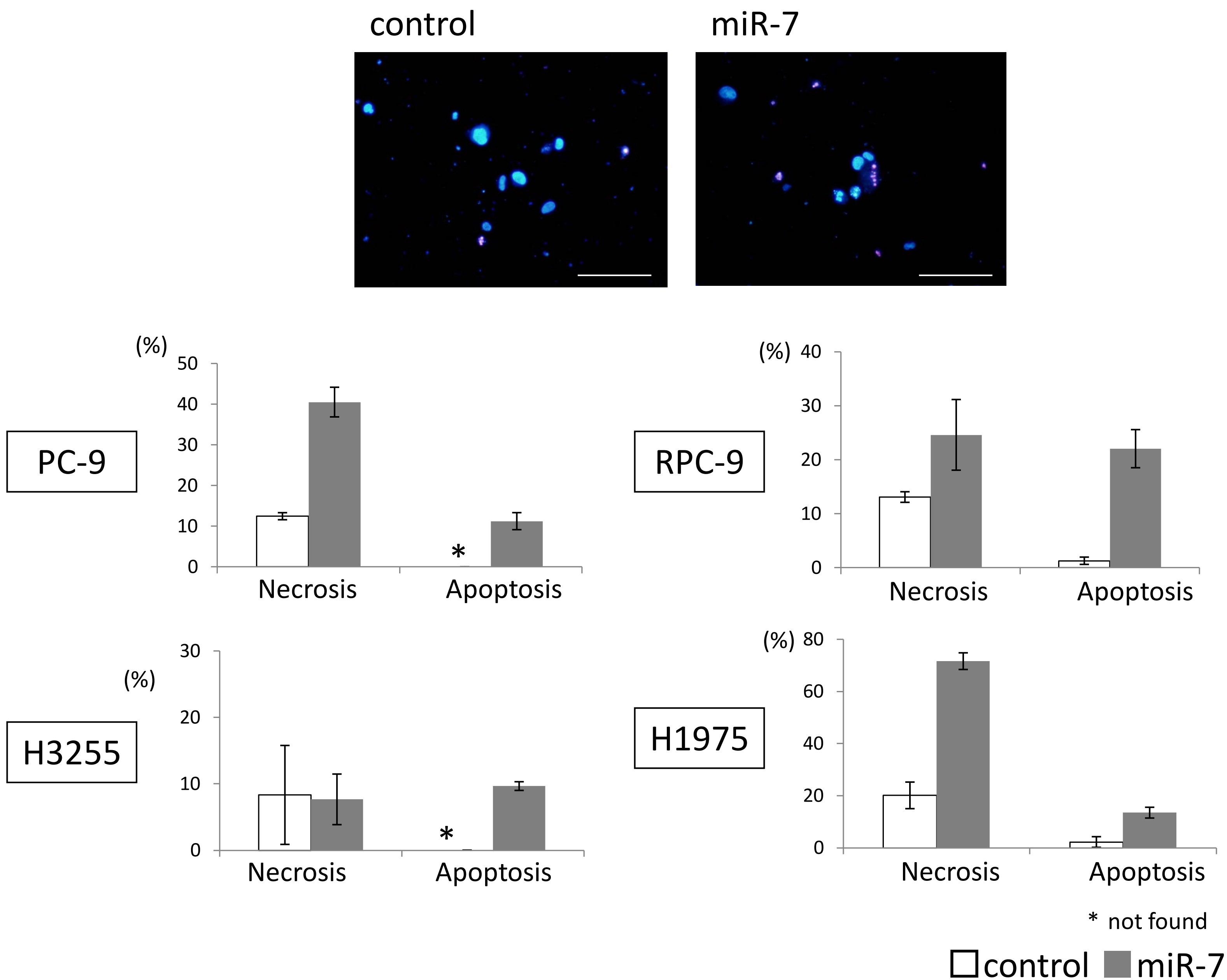

control
miR-7
PC-9
(%)
50
40
30
20
10
0
*
Necrosis
Apoptosis
RPC-9
(%)
40
30
20
10
0
Necrosis
Apoptosis
H3255
(%)
30
20
10
0
*
Necrosis
Apoptosis
H1975
(%)
80
60
40
20
0
Necrosis
Apoptosis
* not found
control
miR-7

Figure S2

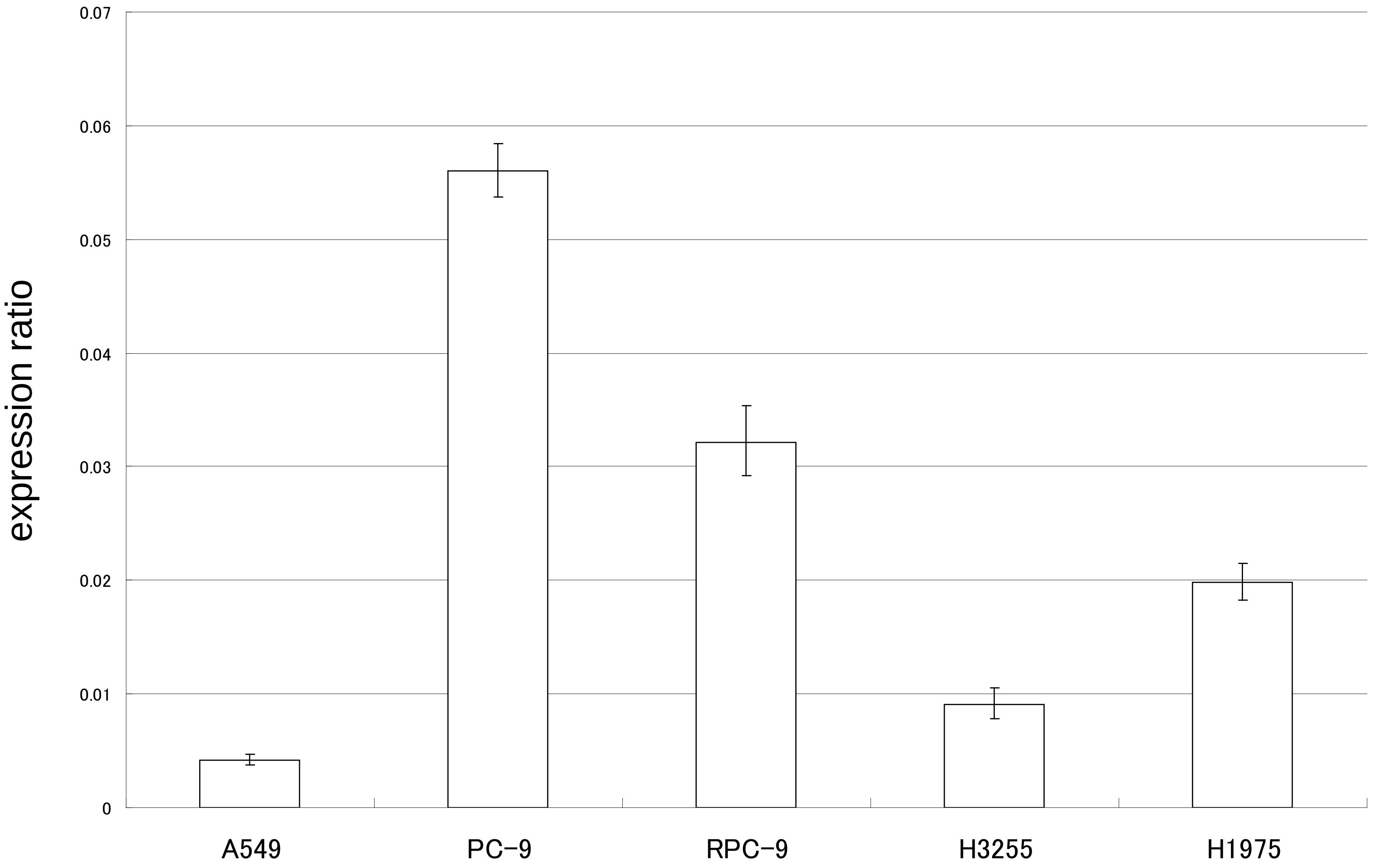
expression ratio
0.07
0.06
0.05
0.04
0.03
0.02
0.01
0
A549
PC-9
RPC-9
H3255
H1975

Figure S2